# Investigations of the galaxies of the LCV

Dimitrios Papachistopoulos

March 24, 2023

## Abstract

The paper investigates the properties of galaxies in the Local Cosmological Volume (LCV), using the Catalogue of Neighboring Galaxies[2] and its updated version from the "Catalog & Atlas of the LV galaxies" database[1]. The properties studied include the galaxy types, their various masses, the star formation rates (SFRs) and the star formation timescale $\tau$, gas depletion timescale $\tau_g$. The paper aims to understand the distribution and correlation of these properties in the sample of galaxies in the LCV, and how they relate to current astrophysical theories. Additionally, the paper discusses the conditions for star formation and the implications of the observed properties on galaxy evolution.

## 1 The Galaxies in the Local Cosmological Volume (LCV)

The Catalogue of Neigbouring Galaxies (Karachentsev, Igor D. and Makarov et al. 2013[2]) and its updated version from the "Catalog & Atlas of the LV galaxies" database[1] are used to extract the B-band, FUV \ K-band luminosities[1] , the types of the galaxie[2]s, the mass within the Holmberg radius (M26), the Hydrogen masses of the galaxies ($M_{HI}$) and the SFRs based on integrated H and far-ultraviolet (FUV) measurments for galaxies within a distance of $\approx$ 11 Mpc. Some of those values contain limit flags, which we exclude from our present analysis. This gives a sample of 793 galaxies from 1248. From the remaing galaxies we have

| | 0 |
|---|---|
| Name | 793 |
| FUVmag | 687 |
| TType | 793 |
| Tdw1 | 580 |
| Tdw2 | 568 |
| Bmag | 790 |
| SFR_Ha | 566 |
| SFR_FUV | 688 |
| K | 789 |
| MHI | 643 |
| color | 686 |

| Measurment | Number of Galaxies |
|---|---|

The K-band values are converted to the total Stellar Masses of each galaxy according to the mass-to-light ratio of 0.6 ([5]), and the $M_{HI}$ can be converted to the total mass of the gas of the galaxy using the equation $M_g = 1.33\, M_{HI}$

The total SFR of each galaxy can be calcuated by

$$SFR_o = \frac{SFR_{FUV} + SFR_{Ha}}{2}$$

if both $SFR_{H\alpha}, SFR_{FUV}$ measurments are available. If only one only one of them is given, then the SFR is equal to the given SFR value

$$SFR_o = SFR_i, \text{ if } SFR_j = 0, i \neq j,\ i, j = FUV, H_a$$

[1] We use the FUV and B measurments to calculate the B-FUV color index.

[2] TType=Morphology type code according to the classification by de Vaucouleurs/ Tdw1=Dwarf galaxy morphology/ Tdw2=Dwarf galaxy surface brightness morphology

The condition $SFR_o \geq 10^{-3} M_{\odot} yr^{-1}$ leaves 579 galaxies. This condition is applied due to the reasons given in the P. Kroupa,M. Haslbauer, I. Banik, S. T. Nagesh and J. Pflamm-Altenburg et al. 2020 [4]

## 2 Types of galaxies

Using the dataset of 1248 galaxies, do before using the condition and removing the galaxies with the flags, the below histograms can be plotted.

Most of the galaxies in the LCV are Higly Irregular galaxies followed by lenticular galaxies

Out of the 1248 galaxies the 1022 are dwarf galaxies

Most dwarf galaxies have low brightness and are irregulars followed by Dwarf spheroidal.

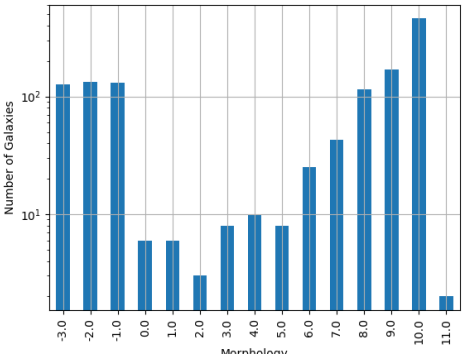


Figure 1: The classification by de Vaucouleurs et al. (1991) is used for the morphology of the galaxies

## 3 Delayed-$\tau$ model

According to P. Kroupa et al. 2020[4] current star formation rates of galaxies can be described by the 'delayed-$\tau$' mode as

$$SFR_{0,del} = \frac{A_{del} x e^{-x}}{\tau}, \text{ where } x = \frac{t_{sf}}{\tau} \quad (1)$$

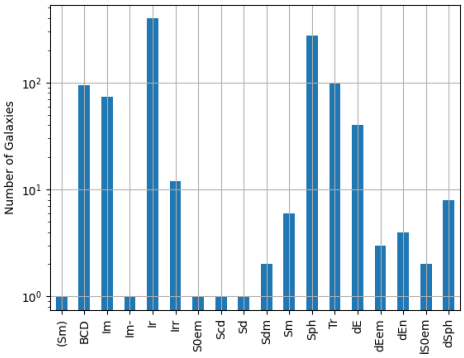


Figure 2: Dwarf galaxy morphology

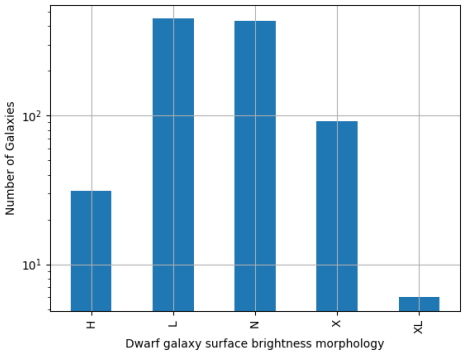


Figure 3: Dwarf galaxy surface brightness morphology, where: H = high; N = normal; L = low; X = extremely low.

where $\tau$ is the star formation time-scale, $t_{sf}$ is the real time of star formation in a given galaxy and $A_{del}$ a normalization constant.

The average SFR is

$$\overline{SFR_{del}} = \frac{A_{del}}{t_{sf}}[1-(1+x)e^{-x}] \tag{2}$$

and can also be defined by the present day stellar mass

$$\overline{SFR} = \frac{\zeta M_*}{t_{sf}} \tag{3}$$

where $\zeta$ accommodates for mass-loss through stella evolution and $\zeta \approx 1.3$

This is a system of 2 equations and 3 variables, since $A_{del}$ has never been calculated

## 3.1 Constant $t_{sf}$

The observed ages of galactic discs are $t_{sf} \approx 12$ Gyr[3], so assuming an approximation of $t_{sf} = 12.5$ Gyr, the $\overline{SFR_{del}}$ can be calcuated, from the equation (**??**).

After that the equation of ratio

$$\frac{\overline{SFR_{del}}}{SFR_{0,del}} = \frac{e^x - x - 1}{x^2} \tag{4}$$

can be solved numerically for $x$ and using the equations (**??**) and (**??**) the $A_{del}$ and $\tau$ of each galaxy are found.

| | A_tsf | tau | x_tsf |
|---|---|---|---|
| count | 5.78E+02 | 5.79E+02 | 5.79E+02 |
| mean | 2.25E+12 | 1.09E+11 | 1.85E+00 |
| std | 3.94E+13 | 1.04E+12 | 1.48E+00 |
| min | 2.48E+07 | 1.93E+09 | 5.59E-04 |
| 25% | 1.41E+08 | 4.18E+09 | 5.65E-01 |
| 50% | 6.84E+08 | 7.79E+09 | 1.60E+00 |
| 75% | 5.70E+09 | 2.21E+10 | 2.99E+00 |
| max | 9.10E+14 | 2.24E+13 | 6.47E+00 |

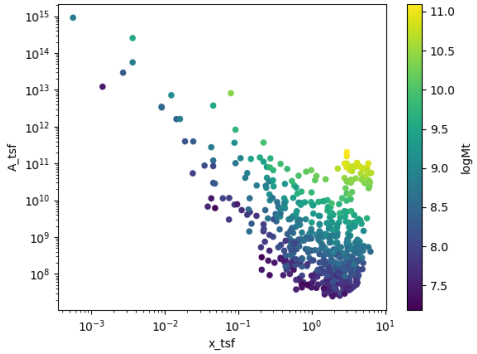


Figure 4: $A_{del} = f(x)$ for constant $t_{sf}$

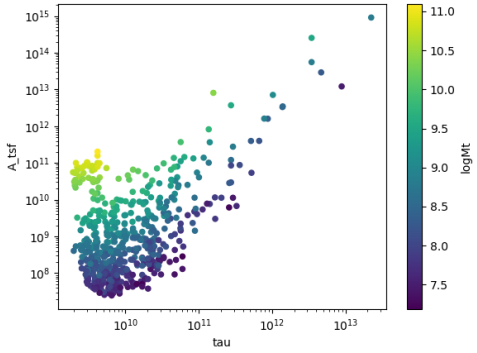


## 3.2 Constant $\tau$

Assuming for an constant $\tau = 3.5$ Gyr, we cannot use the same $\overline{SFR}$ since it depends on $t_{sf}$. Using the equations~(**??**) and (**??**)

$$\frac{\overline{SFR_{del}}}{SFR_{0,del}} = \frac{e^x - x - 1}{x^2} \Leftrightarrow \frac{e^x - x - 1}{x} = \frac{\zeta M_*}{SFR \cdot \tau}$$

using this equation $x$ and $A_{del}$ can be calcuated numerically.

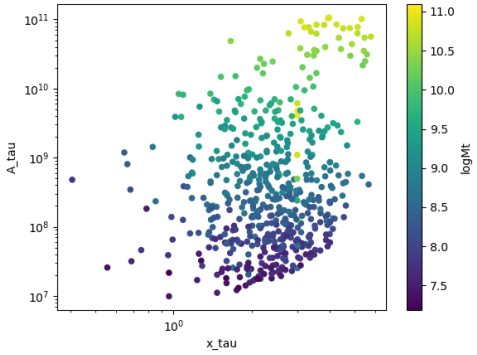


Figure 5: $A_{del} = f(x)$ for constant $\tau$

| | A_tau | x_tau | tsf |
|---|---|---|---|
| count | 5.79E+02 | 5.79E+02 | 5.79E+02 |
| mean | 4.59E+09 | 2.54E+00 | 8.89E+09 |
| std | 1.50E+10 | 9.57E-01 | 3.35E+09 |
| min | 9.87E+06 | 4.07E-01 | 1.42E+09 |
| 25% | 6.50E+07 | 1.87E+00 | 6.55E+09 |
| 50% | 2.37E+08 | 2.44E+00 | 8.54E+09 |
| 75% | 1.12E+09 | 3.08E+00 | 1.08E+10 |
| max | 1.06E+11 | 5.77E+00 | 2.02E+10 |

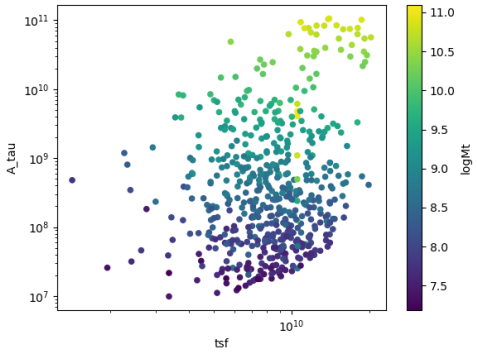


| | x_tau | x_tsf |
|---|---|---|
| count | 5.79E+02 | 5.79E+02 |
| mean | 2.54E+00 | 1.85E+00 |
| std | 9.57E-01 | 1.48E+00 |
| min | 4.07E-01 | 5.59E-04 |
| 25% | 1.87E+00 | 5.65E-01 |
| 50% | 2.44E+00 | 1.60E+00 |
| 75% | 3.08E+00 | 2.99E+00 |
| max | 5.77E+00 | 6.47E+00 |

## 3.3 Comparing the two results

### 3.3.1 Comparing the $x$'s

Comparing the two different results for x, we see that the $x|_\tau$ has a lower $\sigma$

The two results are interrelated through the equation:

$$x|_\tau = (6.30(6) \times 10^{-1}) \cdot x|_{tsf} + (1.374(15) \times 10^{0}) \quad \text{with correlation } R^2 = 94\% \tag{5}$$

and from the plots the following conclusions can be drawn:

1. The galaxies with a higher total mass deviate less from the linear fit and are older.
2. The younger galaxies are mainly later types of galaxies
3. For lower x's, the galaxies have a lower color index which indicates that they are

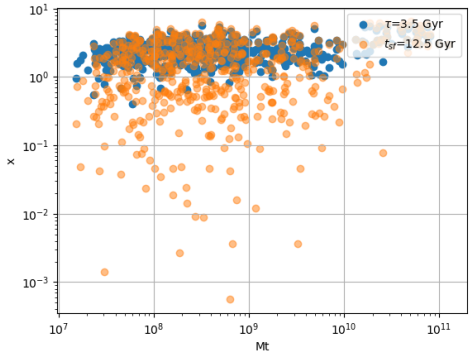


Figure 6: Comparing the two x's, According to their total masses

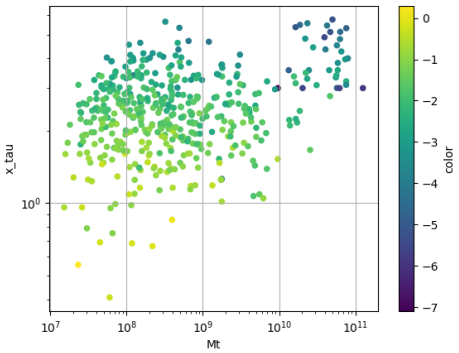


Figure 7: $x|_\tau = f(M_t)$, with their color index

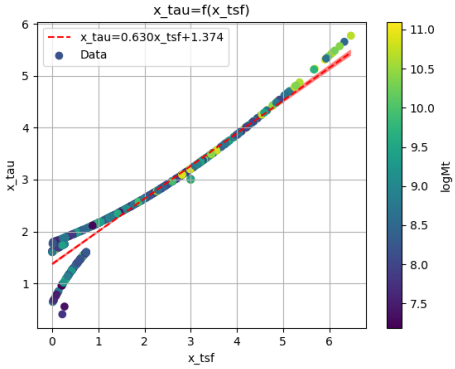


Figure 8: Comparing the two x, according to their total mass

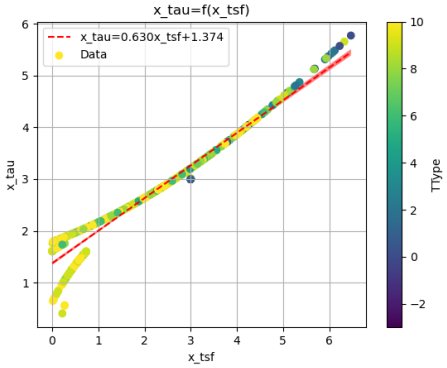


Figure 9: Comparing the two x, according to their type

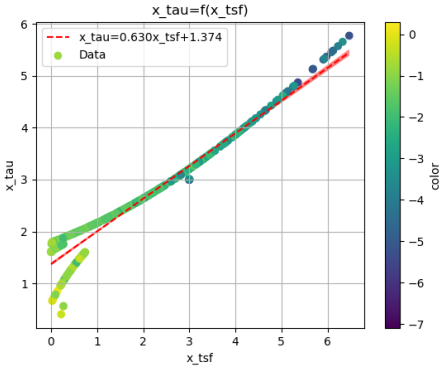


Figure 10: Comparing the two x, according to their color index

younger. So the values are inline with the experimental values.

### 3.3.2 Comparing the normalization constants

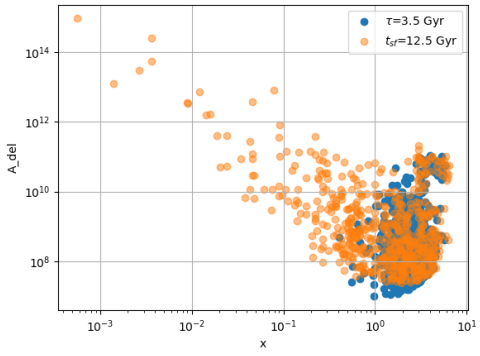


Figure 11: Comparing the two $A_{del}$

For high $x$ and high masses the two $A_{del}$s have a high correlation. Specifically:

1. For high $x$ the $A_{del}|_\tau - A_{del}|_{t_{sf}}$ plot follows a $y = x$ trend, which means that for older stars and stars with a low star formation timescale $\tau$, the normalization constant is the same despite the method used to calculate it.
2. The same is true for more massive galaxies, since they deviate less from the $y = x$ line

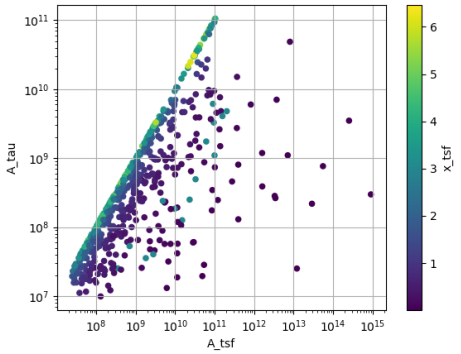


Figure 12: Comparison of the 2 $A_{del}$s according to their $x$

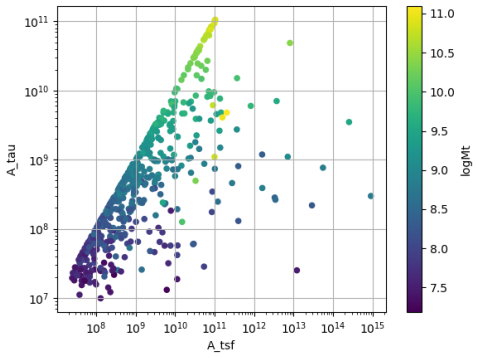


Figure 13: Comparison of the 2 $A_{del}$s according to their total masses

# 4 The gas depletion timescale $\tau_g$

The gas depletion timescale $\tau_g$ measures the time taken by a galaxy to exhaust its gas content Mg given the current SFR[6, 7].

$$\tau_g = \frac{M_g}{\dot{M}_*} = \frac{M_g}{SFR} \tag{6}$$

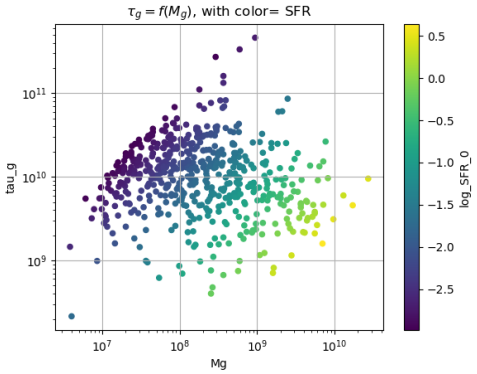


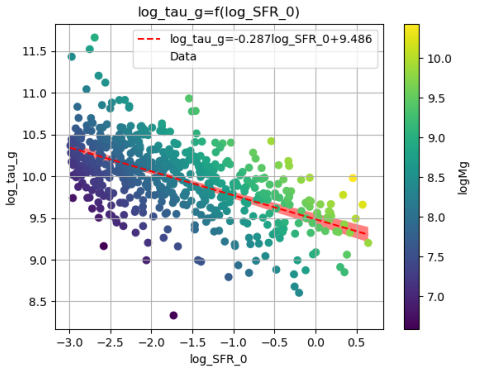


Figure 14: Correlation of the $\tau_g$ with the SFR and the gas mass

Despite a weak logarithmic correlation (as indicated by $R^2 = 32\%$), there is a noticeable trend of decreasing $\tau_g$ with increasing SFR and $M_g$.

The logarithmic correlation between $\tau_g - M_*$ is low ($R^2 = 21\%$), there seems to be a pattern wherein the decrease of $\tau_g$ corresponds to an increase in the values of the Stellar Mass, but there does not seem to be one for $\tau_g - \tau$

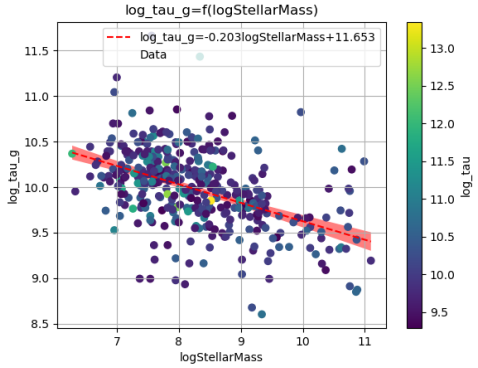


Figure 15: Correlation of the $\tau_g$ with the SFR and the Stellar mass

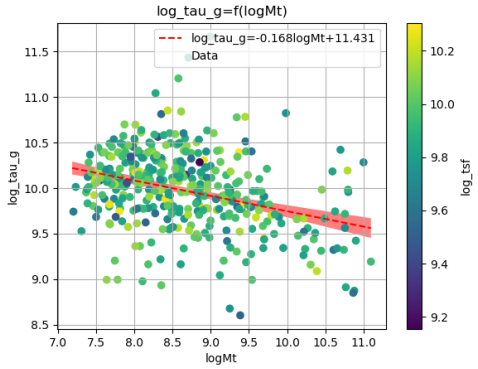


Figure 16: Correlation of the $\tau_g$ with the total mass and the mass of the gas

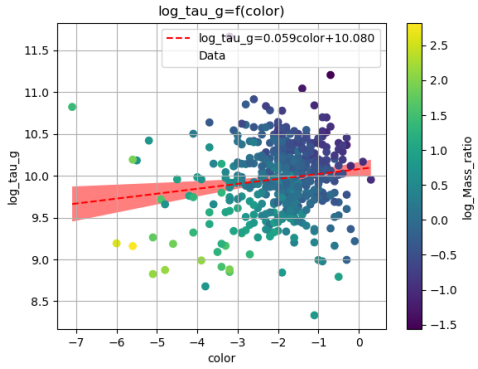


Figure 17: Correlation of the $\tau_g$ with the color index

Again it can be observed that as the $\tau_g$ decreases, the corresponding values of $M_t$ increase, but the logarithmic correlation is again low ($R^2 = 11\%$), and there is no clear correlation between $\tau_g - t_{sf}$

There is a notable trend, wherein for high masses we have a shorter timescale.

# 5 Mass relations

Many of the galaxies masses have a high correlation with each other, and also help us understand the previous calculations.

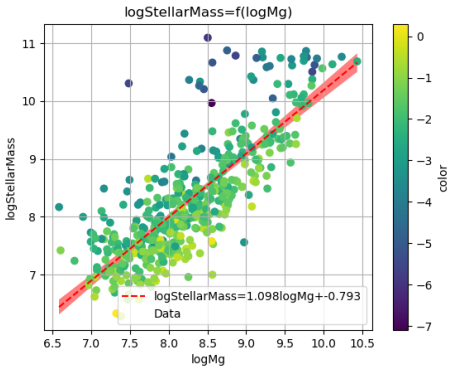


Figure 18: $mg_{SMass}$

For the plot **??**:

$$M_g = (1.098(35) \times 10^0) \cdot M_* + (-7.9(2.9) \times 10^{-1}) \text{ with correlation } R^2 = 64\% \quad (7)$$

For the plot **??**:

$$M26 = (1.076(23) \times 10^0) \cdot M* + (-1.8(1.9) \times 10^{-1}) \text{ with correlation } R^2 = 80\% \quad (8)$$

For the plot **??**:

$$M26 = (1.41(4) \times 10^0) \cdot Mg + (-2.92(30) \times 10^0) \text{ with correlation } R^2 = 74\% \quad (9)$$

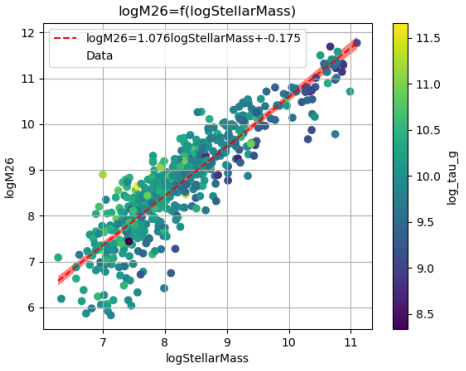


Figure 19: $\text{SMass}_{\text{m26}}$

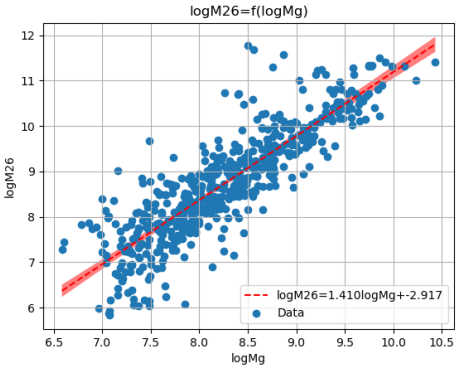


Figure 20: $\text{mg}_{\text{m26}}$

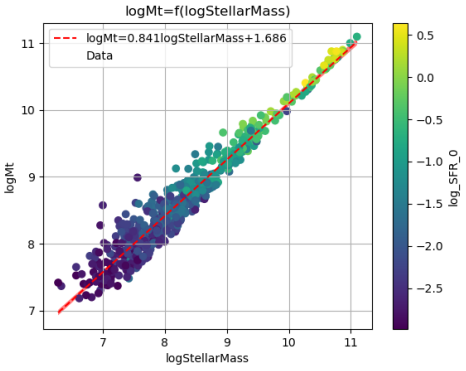


Figure 21: $\text{SMass}_{\text{mt}}$

For the plot **??**:

$$\text{M}_t = (8.41(9)\ \times 10^{-1}) \cdot \text{M}_* + (1.69(8)\ \times 10^{0})$$
$$\text{with correlation } R^2 = 94\% \tag{10}$$

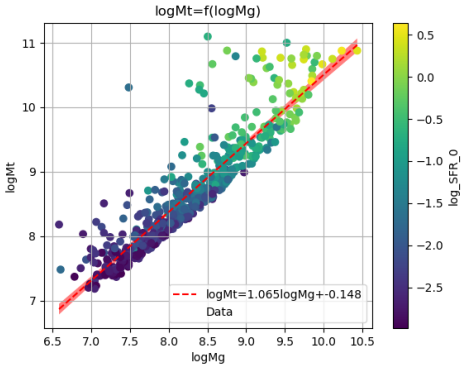


Figure 22: $\text{mg}_{\text{mt}}$

For the plot **??**:

$$\text{M}_t = (1.065(23)\ \times 10^{0}) \cdot \text{M}_g + (\text{-}1.5(1.9)\ \times 10^{-1})$$
$$\text{with correlation } R^2 = 81\% \tag{11}$$

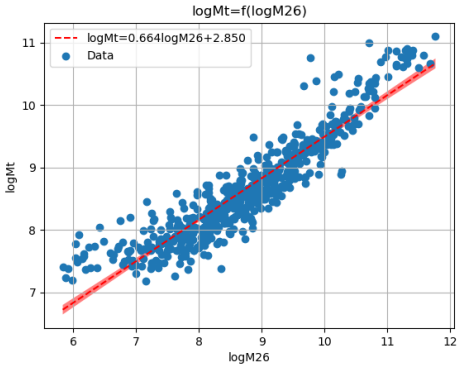


Figure 23: $\text{m26}_{\text{mt}}$

$$M26 = (6.64(12) \times 10^{-1}) \cdot \text{M}_t + (2.85(11)\ \times 10^{0})$$
$$\text{with correlation } R^2 = 85\% \tag{12}$$

There are many plots exhibiting a correlation of $R^2 > 80$

The $M_t - M_*$ (**??**) plot is particularly noteworthy, displaying a correlation of $R^2 = 94\%$. This plot also indicates that galaxies with greater total and stellar masses tend to have higher SFR, consistent with the findings in section **??** where $\tau_g$ decreases with increasing masses.

This phenomenon is likely due to the fact that galaxies with higher masses possess greater potential energy, which accelerates the star formation process. The galaxies with a high Mass ratio $M_r$ could also help the process due to their dense regions and the resulting strong local gravitational potential.

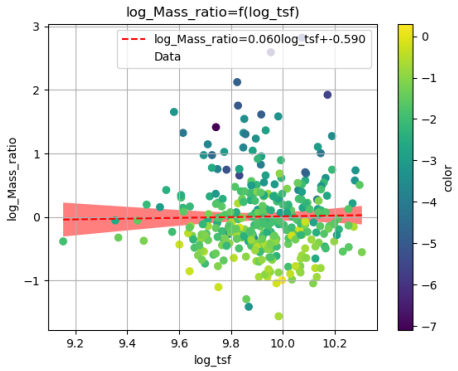


Figure 24: $\text{tsf}_{\text{mr}}$

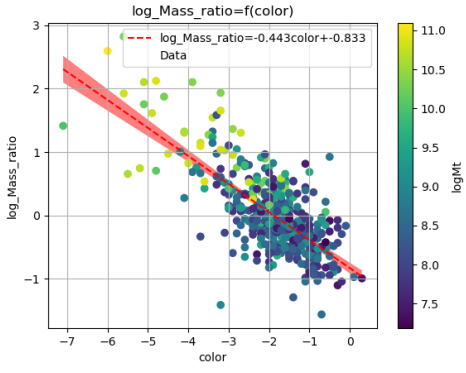


Figure 25: $\text{col}_{\text{Mr}}$

From the **??**, we conclude that when the color index is higher the Mass ratio decreases, which is to be expected, since the higher the B-FUV the more active the star formation of the galaxy.

# 6 Variations in Star Formation Rate Across the Different Masses

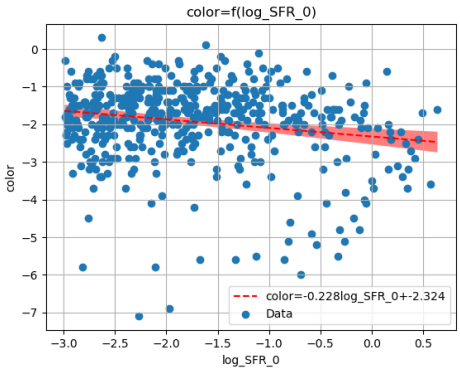


Figure 26: None

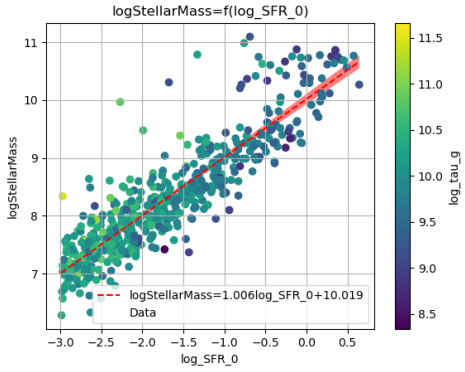


Figure 27: None

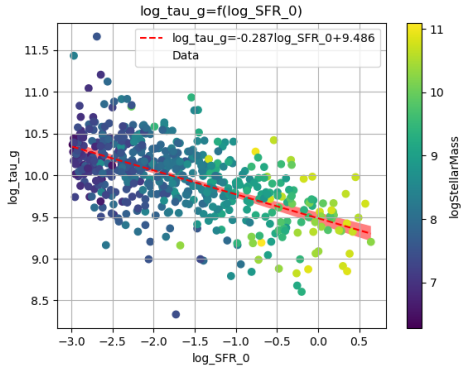


Figure 28: None

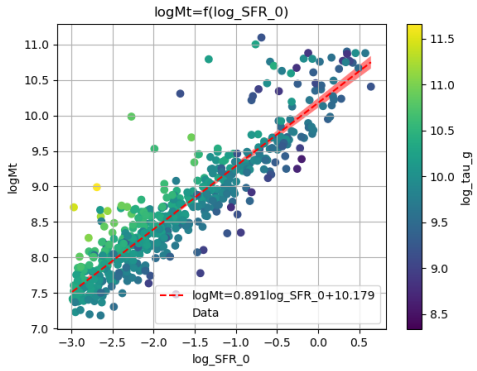


Figure 29: None

# References


[1] *Catalog of the LV Galaxies*. https://www.sao.ru/lv/lvgdb/tables.php. (Visited on 03/13/2023).

[2] Igor D. Karachentsev, Dmitry I. Makarov, and Elena I. Kaisina. "UPDATED NEARBY GALAXY CATALOG". In: *AJ* 145.4 (Mar. 2013), p. 101. ISSN: 0004-6256, 1538-3881. DOI: 10.1088/0004-6256/145/4/101. (Visited on 03/13/2023).

[3] R. A. Knox, M. R. S. Hawkins, and N. C. Hambly. "A Survey for Cool White Dwarfs and the Age of the Galactic Disc". In: *Monthly Notices of the Royal Astronomical Society* 306.3 (July 1999), pp. 736–752. ISSN: 0035-8711. DOI: 10.1046/j.1365-8711.1999.02625.x. (Visited on 03/13/2023).

[4] P Kroupa et al. "Constraints on the Star Formation Histories of Galaxies in the Local Cosmological Volume". In: *Monthly Notices of the Royal Astronomical Society* 497.1 (Sept. 2020), pp. 37–43. ISSN: 0035-8711. DOI: 10.1093/mnras/staa1851. (Visited on 03/13/2023).

[5] Federico Lelli, Stacy S. McGaugh, and James M. Schombert. "SPARC: MASS MODELS FOR 175 DISK GALAXIES WITH SPITZER PHOTOMETRY AND ACCURATE ROTATION CURVES". In: *AJ* 152.6 (Nov. 2016), p. 157. ISSN: 1538-3881. DOI: 10.3847/0004-6256/152/6/157. (Visited on 03/13/2023).

[6] Srikanth T. Nagesh et al. "Simulations of Star-Forming Main-Sequence Galaxies in Milgromian Gravity". In: *Monthly Notices of the Royal Astronomical Society* 519 (Mar. 2023), pp. 5128–5148. ISSN: 0035-8711. DOI: 10.1093/mnras/stac3645. (Visited on 03/13/2023).

[7] Jan Pflamm-Altenburg and Pavel Kroupa. "The Fundamental Gas Depletion and Stellar-Mass Buildup Times of Star Forming Galaxies". In: *ApJ* 706.1 (Nov. 2009). Comment: accepted for publication in ApJ, pp. 516–524. ISSN: 0004-637X,

1538-4357. DOI: 10.1088/0004-637X/706/1/516. arXiv: 0910.1089 [astro-ph]. (Visited on 03/22/2023).